Piezoelectric vortex induced vibration energy harvesting in a random flow field

Sondipon Adhikari

College of Engineering, Swansea University, Bay Campus, Fabian Way, Crymlyn Burrows, Swansea, SA1 8EN, UK

E-mail: S.Adhikari@swansea.ac.uk

Akshat Rastogi

Department of Mechanical Engineering, Indian Institute of Technology Kanpur, India

E-mail: akshat@iitk.ac.in

Bishakh Bhattacharya

Department of Mechanical Engineering, Indian Institute of Technology Kanpur, India

E-mail: bishakh@iitk.ac.in

Submitted June 2019

Abstract. Vibration-based energy harvesters have significant potential for sustainable energy generation from ambience for micro-scale systems like Wireless Sensor Networks and similar low power electronic devices. Vortex-induced vibration (VIV) is one of the richest sources for such power generation for devices installed within a fluid environment. However, uncertainty in the direction and magnitude of the free stream velocity could affect the performance of such systems. We have first developed the mathematical model of a piezoelectric cantilever beam with end mass vibrating under the influence of VIV. The piezo patch is assumed to be in the unimorph and bimorph configurations. From the unimodal dynamic response of the system, an equivalent single degree of freedom mechanical model is developed. This is further integrated with the electrical model of the piezoelectric system without and with an inductor. The energy harvested from the deterministic harmonic excitation is estimated against the non-dimensional velocity parameter. A random process model is developed considering the excitation force due to vortex shedding to be a bounded, weakly stationary and narrowband random process. The power spectral density of the random process is obtained using the Fourier transform of the auto-correlation function. The dynamic response of the energy harvester is obtained against such random excitations. The expressions of the mean power are obtained in closed-form corresponding to the cases without and with the inductor integrated to the electrical circuit. It is observed that while for cases without the inductor, the average harvested power monotonically decreases with increase in damping ratio and decrease in the coupling factor; for models with the inductor, an optimal inductor constant exists corresponding to the maximum mean-power condition. The extensive analytical modelling and initial representative results are expected to pave the way for the practical design of VIV based piezoelectric energy harvesting system subjected to stochastic excitation.

Keywords: Energy harvesting, piezoelectric, vortex induced vibration, stochastic, optimal design

Submitted to: *Smart Materials and Structures*

Nomenclature

Greek Symbols

α dimensionless time constant $\alpha = \omega_n C_p R_l$
α_c, β_c stiffness and mass proportional damping factors
β dimensionless inductor constant $\beta = \omega_n^2 L_i C_p$
ΔM ratio of the tip mass and the mass of the cantilever
γ uniform random variable between 0 to 2π
γ_c a constant for piezoelectric patch (bimorph or unimorph)
κ electromechanical coupling coefficient $\kappa = \theta^2/kC_p$

λ_j natural frequencies of the beam
ν central vortex shedding frequency
Ω dimensionless frequency $\Omega = \omega/\omega_n$
ω frequency
ω_n natural frequency of the harvester
ω_s frequency of vortex shedding
ϕ_j mode shapes of the beam
ρ density of the fluid
ρ_h density of the beam
i unit imaginary number $\mathrm{i} = \sqrt{-1}$
σ strength of the random process
θ electromechanical coupling
$\widehat{c}_1$ strain-rate-dependent viscous damping coefficient
$\widehat{c}_2$ velocity-dependent viscous damping coefficient
ζ damping factor
A cross-section area of the beam
b_c width of the piezoelectric patch
c damping of the harvester
C_L lift coefficient
C_p capacitance of the piezoelectric layer
D diameter of the cylinder
d_{31} constant for piezoelectric material
F_0 non-dimensional forcing amplitude $F_0 = \frac{1}{2}u^2\frac{C_L}{M_r}$
$f_L(t)$ vortex induced forcing to the harvester
h thickness of the beam
h_c thickness of the piezoelectric patch
I second-moment of the cross-section of the beam
k equivalent stiffness of the harvester
L length of the beam
L_c length of the piezoelectric patch
L_i inductance
m equivalent mass of the harvester
M_r dimensionless relative mass $M_r = m/\rho D^3$
R_l load resistance
S Strouhal number
t time
U free stream velocity
u non-dimensional free stream velocity $u = U/D\omega_n$
$V(\mathrm{i}\omega)$ Fourier transform of voltage $v(t)$
$v(t)$ voltage
$W(t)$ standard Wiener process
W_c work done by the piezoelectric patch
$Y(\mathrm{i}\omega)$ Fourier transform of displacement $y(t)$
$y(t)$ displacement of the mass
$Z(x,t)$ transverse displacement of the beam

Other Variables

$(\bullet)^*$ complex conjugation
$|\bullet|$ absolute value
$\det \bullet$ determinant of a matrix
$\mathrm{E}[\bullet]$ expectation operator
$\Phi_\bullet(\omega)$ power spectral density
$R_\bullet$ autocorrelation function

1. Introduction

Researchers over the years have been trying different ways to prepare for the energy-intensive lifestyle of mankind in future. Significant research has been performed on harnessing energy present in the environment

such as kinetic energy of the wind, thermal energy which is abundant in tropical countries, high velocity of river water using which dams extract energy etc. The energy harvesting can be implemented on micro or macroscale depending on the application and the power consumption. Of the micro-scale systems, the vibration dependent energy harvesters, typically based on piezoelectric materials, are most common where the cause of vibration is the differentiating factor. In this paper, we consider the energy harvesting from a cantilever beam with a piezo patch where the source of vibration is the vortex shedding in the wake of a bluff body attached at the free-end of the cantilever beam (Park *et al* [1]).

Broadly, there are two approaches to model a vortex induced vibration problem. First is formulating it by using the fluid mechanics intensive Computational Fluid Dynamics (CFD) approach while the other is using the phenomenological models to simulate the behaviour of vortex shedding. In the CFD based approach, formulations like arbitrary Lagrangian-Eulerian (Hirt *et al* [2]), immersed boundary method (Wang [3]), accelerated reference frame method (Mehmood *et al* [4]), moving immersed boundary method (Cai *et al* [5]) and spectral methods (Soti *et al* [6], Yieser [7]) have been used. Due to the inherent complexity of the Navier Stokes equations and high computational requirements, researchers have used phenomenological models to simulate and study the inherent behaviour of the vortex shedding phenomenon. Of the phenomenological models, there are two approaches for studying VIV depending upon whether the feedback effect is incorporated or not. The simple linear harmonic model (Blevins [8]), also called the forced model by Païdoussis *et al* [9], does not incorporate the feedback effect while there are coupled nonlinear models such as wake oscillator model which do. The wake oscillator models predict the self-limiting and self-exciting characteristics (de Langre [10]) of the shedding phenomenon. Bishop and Hassan [11] first suggested the use of Van der Pol oscillator in modelling the behaviour of the vortex shedding. Tamura and Matsui [12] proposed the Birkhoff model for modelling vortex shedding phenomenon for circular cylinders. Amongst all the wake oscillator models, the most commonly used is Van der Pol oscillator which has been studied and refined over the years (see for example Skop and Balasubramaniam [13]) to match closely with the physical vortex shedding phenomenon. Facchinetti *et al* [14] analyzed coupled models (displacement, velocity, acceleration coupling) and demonstrated that the acceleration coupling closely simulates the VIV principle by matching the behaviour near lock-in with the experimental results. Benaroya *et al* [15] provided a variational based approach to study the fluid-solid interaction problem. Farshidianfar and Zanganeh [16] modelled the structural oscillator also as a Van der Pol oscillator reasoning that the model then accounts for the compliance with a wide range of mass ratios. Gabbai and Benaroya [17] in their review paper gave an overview of VIV for circular cylinders. Several authors (Pavlovskaia *et al* [18], Hoebeck and Inman [19], Bourguet *et al* [20]), Antoine *et al* [21]) have extended the single degree of freedom formulation of Van der Pol oscillator to a continuous system such as a flow across a long cylinder or cables and Wu *et al* [22] reported a review paper on the same.

On a macro scale, it is the role of the designers and engineers to curb the harmful effect of the fluid-solid interaction phenomenon as large amplitude motion of the structure may cause serious damage. On micro-scale, the same phenomenon can be advantageous in the sense that it can be used to harvest the energy arising out of the vibration of the structure. Dai *et al* [23] mounted a bluff body at the end of a piezoelectric beam and performed nonlinear analysis to determine the number of modes needed to evaluate the performance of harvester. Mehmood *et al* [4] discuss the energy harvesting from vortex induced vibration of a cylinder in the regime of $96 \leq Re \leq 118$ and also incorporates the effect of load resistance. The results show that there is an optimum resistance for which the harvested energy is maximum. Soti *et al* [6] considered the energy harvesting from the VIV of a cylinder and used a conducting coil in a magnetic field to harness the energy from vibration. Hu *et al* [24] showed the means to increase the unstable range of VIV by attaching two thin rods at circumferential location of $\theta = 60^\circ$ on either side of the cylinder while Zhang *et al* ([25], [26]) used an interference cylinder of various shapes [25] and nonlinear magnetic forces [26] to enhance the harvested power in VIV.

Extensive work has been done on studying other mechanisms of energy harvesting from flow-induced vibrations. Li *et al* [27], Hamlehdar *et al* [28], Daqaq *et al* [29], Zhao and Yang [30] and Abdelkefi [31] in a review paper discuss the existing research on harvesting energy from flow-induced vibration mechanisms such as VIV, turbulence induced vibration, galloping and wake galloping. Hoebeck and Inman [19] discuss the energy harvesting from a lightweight and highly robust piezoelectric grass subjected to turbulence induced vibration. Petrini and Gkoumas [32] discuss the energy harvesting from the vibration arising due to the simultaneous effect of vortex shedding and galloping. Shan *et al* [33] have shown energy harvesting from micro-fibre piezoelectric energy harvester placed in the wake of a vibrating cylinder in water flow.

Although extensive research has been carried out on harvesting power from VIV of a bluff body such as a cylinder in a steady and uniform flow field, not much focus has been given on the randomness which may

occur in the flow field. It is important in the context since although we can guarantee a constant flow field in a laboratory setup, this cannot be ensured in real-life situations. There will be inherent variabilities associated with naturally occurring fluid flow, which in turn acts as the main excitation to the energy harvester. This paper develops new approaches for energy harvesting from vortex induced vibration when the flow is random in nature. The dynamics of cantilever energy harvesters with a bluff-body at the tip and reduced-order modelling approaches are discussed in Section 2 (further details are in the Appendix). Piezo patch with unimorph and bimorph configurations have been employed. In Section 3, the single-degree-of-freedom electromechanical model is briefly reviewed, basic equations describing the system are derived and key non-dimensional parameters are introduced. The random process model describing the fluid flow is introduced in Section 4. General approaches to obtain the mean of the harvested power due to random flow are outlined in Section 5. Analytical methods to quantify harvested power are developed in Section 6. A closed-form expression of average harvested power for systems without an inductor is derived in Subsection 6.1, while the same quantity for systems with an inductor is derived in Subsection 6.2. The analytical expressions derived in the paper are numerically applied to illustrative problems. Based on this study, the main conclusions are drawn in Section 7.

2. Model-order reduction for vibration energy harvesters

2.1. The partial differential equation

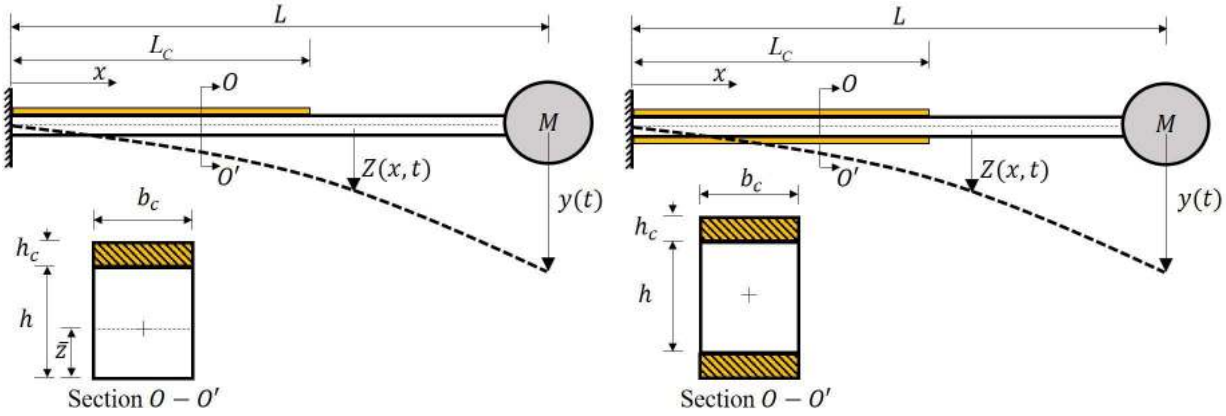

(a) Unimorph harvester (b) Bimorph harvester

Fig. 1. Cantilever vibration energy harvesters with unimorph and bimorph configurations. The length of the cantilever is L and the mass of the bluff body attached at the tip is M.

Vibration energy harvesters are often implemented as a cantilever beam with a piezoelectric patch and a mass attached at the tip of the beam [34]. Due to the small thickness to length ratio, Euler-Bernoulli beam theory is generally used to model bending vibration of such cantilevers. The equation of motion of free-vibration of a damped cantilever modelled (see for example [35]) using Euler-Bernoulli beam theory can be expressed as

$$EI\frac{\partial^4 Z(x,t)}{\partial x^4} + \widehat{c}_1\frac{\partial^5 Z(x,t)}{\partial x^4 \partial t} + \rho_h A\frac{\partial^2 Z(x,t)}{\partial t^2} + \widehat{c}_2\frac{\partial Z(x,t)}{\partial t} = 0 \tag{1}$$

In the above equation x is the coordinate along the length of the beam, t is the time, E is the Young's modulus, I is the second-moment of the cross-section, A is the cross-section area, ρ_h is the density of the material and $Z(x,t)$ is the transverse displacement. The length of the beam is assumed to be L. Additionally $\widehat{c}_1$ is the strain-rate-dependent damping coefficient, $\widehat{c}_2$ is the velocity-dependent viscous damping coefficient. The strain-rate-dependent damping can be used to model inherent damping property of the material of the cantilever beam. The velocity-dependent viscous damping can be used to model damping due to external factors such as a cantilever immersed in a fluidic environment. The present model uses only an isotropic material property for the beam. Anisotropic/orthotropic materials, such as composite materials, are increasingly being used along with piezoelectric transducers for vibration energy harvesting. In order to incorporate such advanced materials, different equations will be necessary. However, the reduced-order model in those cases (anisotropic/orthotropic) would follow an approach similar to what is to be presented here.

Schematic diagram of cantilever vibration energy harvesters with unimorph and bimorph configurations are shown in Fig. 1. An equivalent single-degree-of-freedom (SDOF) model can be obtained from this equation. The necessary details are given in the Appendix.

2.2. The electromechanical coupling

Equivalent mass, damping and stiffness considering the first mode of vibration can be obtained following the approach in the Appendix. The analysis presented there does not incorporate any piezoelectric effect. Here we will take this into account. Suppose that piezoelectric layers added to a beam is either in a unimorph or a bimorph configuration as shown in Fig. 1. Then the moment about the beam neutral axis produced by a voltage V across the piezoelectric layers may be written as

$$M(x,t) = \gamma_c V(t) \tag{2}$$

The constant γ_c depends on the geometry, configuration and piezoelectric device and $V(t)$ is the time-dependent voltage. For a bimorph as in Fig. 1(b), with piezoelectric layers in the 31 configuration, with thickness h_c, width b_c and connected in parallel

$$\gamma_c = E d_{31} b_c \left(h + h_c\right) \tag{3}$$

Here h is the thickness of the beam and d_{31} is the piezoelectric constant. For an unimorph as in Fig. 1(a), the constant is

$$\gamma_c = E d_{31} b_c \left(h + \frac{h_c}{2} - \bar{z}\right) \tag{4}$$

where $\bar{z}$ is the effective neutral axis. These expressions assume a monolithic piezoceramic actuator perfectly bonded to the beam.

The work done by the piezoelectric patches in moving or extracting the electrical charge is

$$W_c = \int_0^{L_c} M(x,t)\kappa_c(x)\mathrm{d}x \tag{5}$$

where L_c is the active length of the piezoelectric material, which is assumed to be attached at the clamped end of the cantilever beam. The quantity $\kappa_c(x)$ is the curvature of the beam and this is approximately expressed by the second-derivative of the displacement. Using the approximation for κ_c we have

$$W_c = \theta V \tag{6}$$

where the coupling coefficient

$$\theta = \gamma_c \int_0^{L_c} \frac{\partial^2 \phi(x)}{\partial x^2}\mathrm{d}x \tag{7}$$

Considering the change to the non-dimensional variable in equation (A.4) and noting that we have the second-order derivative within an integral, the above equation can be simplified as

$$\theta = \frac{\gamma_c}{L}\phi'(\xi_c) \tag{8}$$

where $\xi_c = L_c/L$ is the fraction of the length of the piezo patch. Using the first mode shape, as an example when the piezo patch covers the full length of the beam, this can be evaluated as

$$\phi'(1) = \frac{2\lambda\ \left(\cos\left(\lambda\right)\sinh\left(\lambda\right) + \cosh\left(\lambda\right)\sin\left(\lambda\right)\right)}{\cosh\left(\lambda\right) + \cos\left(\lambda\right)} \tag{9}$$

3. The electromechanical model of the energy harvester

Various types of piezoelectric harvesting devices are available, integrating stack or patch transducers. Often these can be represented mechanically as a single degree of freedom system, particularly when the excitation is band-limited and the natural frequencies are well separated. In this paper, we use a beam type harvester with a tip mass (in unimorph and bimorph configuration) as shown in Fig. 2. The tip mass is a cylinder that acts a bluff body when placed in a running fluid to produce vortex induced vibration in the system. The tip mass not only produces the effect of shedding of vortices in its wake but also increases the strain

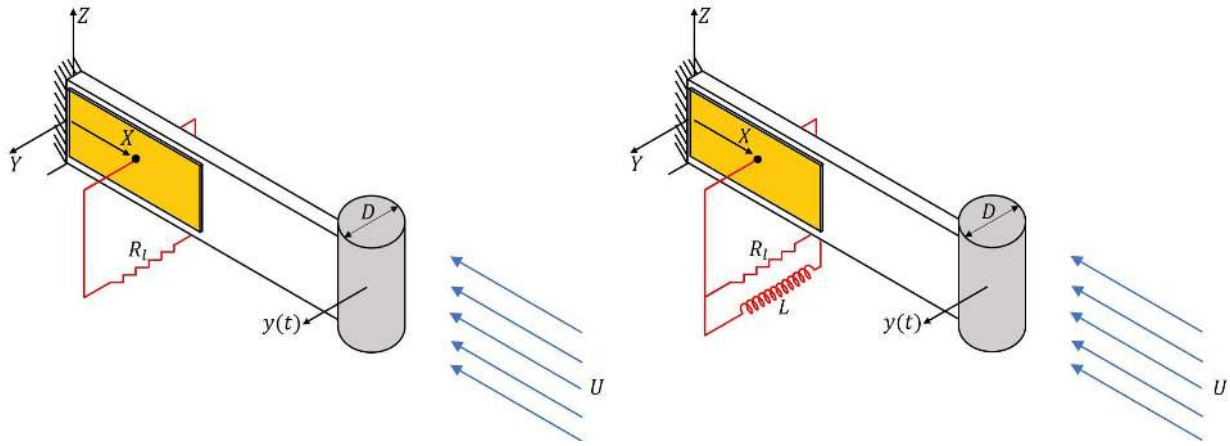

(a) Harvesting circuit without an inductor (b) Harvesting circuit with an inductor

Fig. 2. Schematic diagrams of vortex-induced piezoelectric vibration energy harvesters with two different harvesting circuits.

in the piezoelectric material and the separation between the first and second natural frequencies. The two typical types of circuits used in this paper, namely without and with an inductor, are shown in Fig. 2(a) and Fig. 2(b) respectively. A more detailed model of the cantilever beam harvester, along with correction factors for a single degree of freedom model that accounts for distributed mass effects, was given by Erturk and Inman [36, 37, 38, 39]. This enables the analysis described here to be used in a wide range of practical applications, providing that the vortex-induced vibration does not excite higher vibration modes of the harvester. The single degree of freedom model could be extended to multi-degree of freedom mechanical systems by using a modal decomposition of the response.

3.1. Circuit without an inductor

The coupled electromechanical behaviour of the energy harvester [34] within the fluid flow can be expressed (see, for example [40, 41]) by linear ordinary differential equations as

$$m\ddot{y}(t) + c\dot{y}(t) + ky(t) - \theta v(t) = f_L(t) \tag{10}$$

$$C_p\dot{v}(t) + \frac{1}{R_l}v(t) + \theta\dot{y}(t) = 0 \tag{11}$$

The mechanical part of equation (10) is simply the single degree of freedom (SDOF) model in (A.14) with $y(t) = z_j(t)$ and

$$m = \rho_h AL\left(I_1 + \Delta M\, I_3\right), k = \frac{EI}{L^3}I_2 \quad \text{and} \quad \theta = \frac{\gamma_c}{L}I_4 \tag{12}$$

Here the integrals are given by

$$I_1 = \int_0^1 \phi^2(\xi)\mathrm{d}\xi, I_2 = \int_0^1 \phi^{''2}(\xi)\mathrm{d}\xi, I_3 = \phi^2(1) \quad \text{and} \quad I_4 = \phi'(\xi_c) \tag{13}$$

where $\phi(\xi)$ is the assumed displacement shape expressed as a function of the non-dimensional length ξ. In equation (10), $f_L(t)$ is the applied force on the SDOF harvester due to vortex shedding. This forcing will be considered random in this paper. The electrical load resistance is R_l and the mechanical force is modelled as proportional to the voltage across the piezoceramic, $v(t)$. Equation (11) is obtained from the electrical circuit, where the voltage across the load resistance arises from the mechanical strain through the electromechanical coupling, θ, and the capacitance of the piezoceramic, C_p.

In equation (10), the lift force due to vortex shedding [8] is given by

$$f_L(t) = \frac{1}{2}\rho U^2 DC_L\cos(\omega_s t) \tag{14}$$

where ρ is the fluid density, U is the free stream velocity, D is the diameter of the cylinder, C_L is the non-dimensional lift coefficient. Here ω_s is circular frequency of vortex shedding, which can be expressed as

$$\omega_s = 2\pi f_s, \quad \text{where} \quad f_s = \frac{SU}{D} \tag{15}$$

where S is the Strouhal number. For a cylindrical shape, this is normally between 0.2 - 0.3 [8].

For the initial discussion we consider deterministic harmonic excitation so that

$$f_L(t) = \frac{1}{2}\rho U^2 D C_L e^{\mathrm{i}\omega t} \tag{16}$$

Here ω is the driving frequency which has the same mathematical form as given by (15). Transforming equations (10) and (11) into the frequency domain and dividing the first equation by m and the second equation by C_p we obtain

$$\left(-\omega^2 + 2\mathrm{i}\omega\zeta\omega_n + \omega_n^2\right) Y(\mathrm{i}\omega) - \frac{\theta}{m} V(\mathrm{i}\omega) = \frac{1}{2}\frac{U^2 C_L}{D^2 M_r} \tag{17}$$

$$\mathrm{i}\omega\frac{\theta}{C_p} Y(\mathrm{i}\omega) + \left(\mathrm{i}\omega + \frac{1}{C_p R_l}\right) V(\mathrm{i}\omega) = 0 \tag{18}$$

Here $Y(\mathrm{i}\omega)$ and $V(\mathrm{i}\omega)$ are respectively the Fourier transforms of $y(t)$ and $v(t)$. The natural frequency of the harvester (ω_n), the damping factor (ζ) and the relative mass are defined as

$$\omega_n = \sqrt{\frac{k}{m}} \quad \zeta = \frac{c}{2m\omega_n}, \quad \text{and} \quad M_r = \frac{m}{\rho D^3} \tag{19}$$

Dividing the equation (17) by ω_n^2 and equation (18) by ω_n and writing in a matrix form one has

$$\begin{bmatrix} \left(1-\Omega^2\right) + 2\mathrm{i}\Omega\zeta & -\frac{\theta}{k} \\ \mathrm{i}\Omega\frac{\alpha\theta}{C_p} & (\mathrm{i}\Omega\alpha + 1) \end{bmatrix} \begin{Bmatrix} Y(\mathrm{i}\Omega) \\ V(\mathrm{i}\Omega) \end{Bmatrix} = \begin{Bmatrix} \frac{1}{2}u^2\frac{C_L}{M_r} \\ 0 \end{Bmatrix} = \begin{Bmatrix} F_0 \\ 0 \end{Bmatrix} \tag{20}$$

Here the non-dimensional forcing amplitude, the non-dimensional free stream velocity, the dimensionless frequency and the dimensionless time constant are defined as

$$F_0 = \frac{1}{2}u^2\frac{C_L}{M_r}, \quad u = \frac{U}{D\omega_n}, \quad \Omega = \frac{\omega}{\omega_n} \quad \text{and} \quad \alpha = \omega_n C_p R_l \tag{21}$$

α is the time constant of the first order electrical system, non-dimensionalized using the natural frequency of the mechanical system. Inverting the coefficient matrix, the displacement and voltage in the frequency domain can be obtained as

$$\begin{Bmatrix} Y(\mathrm{i}\Omega) \\ V(\mathrm{i}\Omega) \end{Bmatrix} = \frac{1}{\Delta_1(\mathrm{i}\Omega)} \begin{bmatrix} (\mathrm{i}\Omega\alpha + 1) & \frac{\theta}{k} \\ -\mathrm{i}\Omega\frac{\alpha\theta}{C_p} & \left(1-\Omega^2\right) + 2\mathrm{i}\Omega\zeta \end{bmatrix} \begin{Bmatrix} F_0 \\ 0 \end{Bmatrix} = \begin{Bmatrix} (\mathrm{i}\Omega\alpha + 1)\, F_0/\Delta_1(\mathrm{i}\Omega) \\ -\mathrm{i}\Omega\frac{\alpha\theta}{C_p} F_0/\Delta_1(\mathrm{i}\Omega) \end{Bmatrix} \tag{22}$$

where the determinant of the coefficient matrix is

$$\Delta_1(\mathrm{i}\Omega) = (\mathrm{i}\Omega)^3\alpha + (2\,\zeta\,\alpha + 1)\,(\mathrm{i}\Omega)^2 + \left(\alpha + \kappa^2\alpha + 2\,\zeta\right)(\mathrm{i}\Omega) + 1 \tag{23}$$

and the non-dimensional electromechanical coupling coefficient is

$$\kappa^2 = \frac{\theta^2}{kC_p} \tag{24}$$

It is convenient to view the response quantities in a non-dimensional form. This can be achieved in various ways. Here we propose to non-dimentionalise the dynamic response with the response at zero frequency, that is, with the static force. This quantity can be obtained form equation (22) as

$$Y_0 = Y(\mathrm{i}\Omega)|_{\Omega=0} = F_0 \tag{25}$$

Therefore, the non-dimensional dynamic response is given by

$$\widehat{Y}(\mathrm{i}\Omega) = \frac{Y(\mathrm{i}\Omega)}{Y_0} = \frac{\mathrm{i}\Omega\alpha + 1}{\Delta_1(\mathrm{i}\Omega)} \tag{26}$$

The harvested power is given by

$$P(\Omega) = \frac{V^2(\Omega)}{R_l} \tag{27}$$

As R_l is a constant, to obtain an expression of the power in a non-dimensional form, it is necessary to non-dimentionalise the voltage. Again, several choices are possible. For analytical convenience, the voltage at $\Omega = 1$ when the damping is zero is considered to be used for the normalisation

$$V_0 = V(\mathrm{i}\Omega)|_{\{\Omega=1,\zeta=0\}} = \frac{-\mathrm{i}\frac{\alpha\theta}{C_p}F_0}{\mathrm{i}\alpha\kappa^2} = \frac{-\frac{\alpha\theta}{C_p}F_0}{\alpha\kappa^2} \tag{28}$$

Using this, we obtain the non-dimensional voltage response as

$$\widehat{V}(\mathrm{i}\Omega) = \frac{V(\mathrm{i}\Omega)}{V_0} = \alpha\kappa^2\frac{\mathrm{i}\Omega}{\Delta_1(\mathrm{i}\Omega)} \tag{29}$$

The non-dimensional power is therefore given by

$$\widehat{P}(\Omega) = \frac{P(\Omega)}{P_0} = \left|\widehat{V}(\mathrm{i}\Omega)\right|^2 \tag{30}$$

For the case of deterministic excitation, a key interest is the variation of the dynamic response of the harvester and harvested power as function of the free stream velocity. The non-dimensional frequency parameter Ω can be related to the non-dimensional velocity parameter u as

$$\Omega = \frac{\omega}{\omega_n} = 2\pi\frac{SU}{D\omega_n} = 2\pi Su \tag{31}$$

To gain physical insights, the results obtained so far is applied numerically to an example problem. Table 1 gives the parameters of the system for the simulations. In Fig. 3, the non-dimensional displacement amplitude

Table 1. Parameter values used in the simulation

Parameter	**Value**	**Unit**
m	17.0×10^{-3}	kg
k	4.1×10^{3}	N/m
c	0.218	Ns/m
R_l	3×10^{4}	Ohm
C_p	4.3×10^{-8}	F
θ	-4.57×10^{-3}	N/V
D	19.8×10^{-3}	m
ρ	1×10^{3}	kg/m^3
C_L	1	–
M_r	2.19	–
S	0.2	–
α	0.8649	–
κ^2	0.1185	–

of the harvester given by equation (26) is plotted as function of the non-dimensional free-stream velocity u. The non-dimensional harvested power given by equation (30) is plotted as a function of the non-dimensional free-stream velocity u in Fig. 4. For both quantities, five values of the damping factors of energy harvesters have been considered. As expected, less damping in the harvester leads to more harvested power from the vortex induced vibration. For lightly damped systems, the harvested power peaks about $\Omega \approx 1$. A mathematical optimisation analysis shows that the optimal value of the non-dimensional frequency for the maximum power is given by

$$\Omega^2_{\max} \approx \frac{1 - \left(\kappa^2 - 1\right)\alpha^2}{1 - \left(2\,\kappa^2 - 1\right)\alpha^2} \gtrsim 1 \tag{32}$$

Therefore, from equation (31), the non-dimensional velocity for maximum harvested power is obtained as

$$u_{\max} = \frac{\Omega_{\max}}{2\pi S} \tag{33}$$

The non-dimensional velocity for the maximum harvested power is therefore a function of the Strouhal number, dimensionless time constant and electromechanical coupling coefficient *only*. Therefore, $u_{\max}$ is

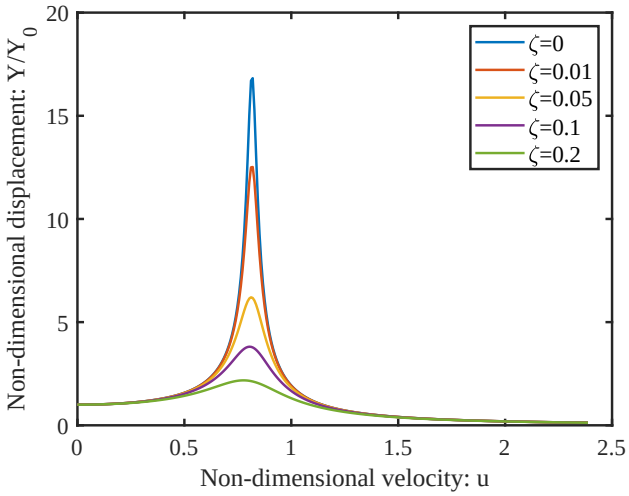

Fig. 3. The non-dimensional displacement amplitude of a harvester without an inductor as a function of the non-dimensional free stream velocity for five selected values of damping factors.

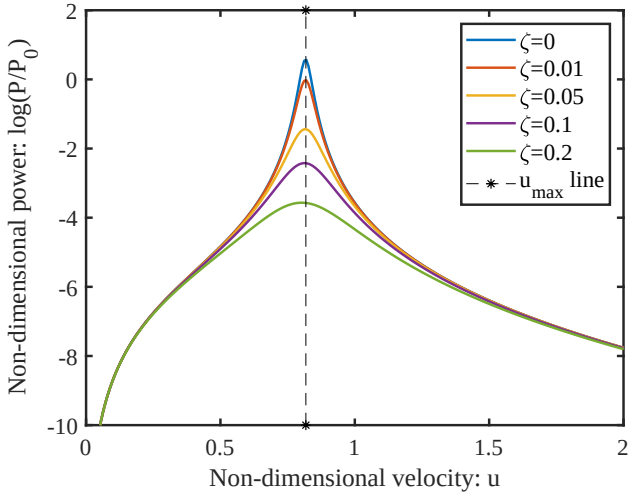

Fig. 4. The non-dimensional power of a harvester without an inductor as a function of the non-dimensional free stream velocity for five selected values of damping factors.

effectively a fixed value for a chosen circuit and the shape of the bluff body. One should adjust the tip mass such that $\Omega_{\max}$ obtained from equation (32) matches with a given design flow velocity. The value of $u_{\max}$ obtained from equation (33) is shown in Fig. 4 by a '*'. It can be observed that it closely matches with the flow velocity for which the harvested power is maximum for all the five damping values.

3.2. Circuit with an inductor

Piezoelectric vibration energy harvester comprising a circuit with an inductor is shown in Fig. 2(b). For this case the electrical equation (see for example, [42]) becomes

$$C_p\ddot{v}(t) + \frac{1}{R_l}\dot{v}(t) + \frac{1}{L_i}v(t) + \theta\ddot{y}(t) = 0 \tag{34}$$

where L_i is the inductance of the circuit. The mechanical equation is the same as given in equation (10).

Transforming equation (34) into the frequency domain and dividing by $C_p\omega_n^2$ one has

$$-\Omega^2\frac{\theta}{C_p}Y(\mathrm{i}\omega) + \left(-\Omega^2 + \mathrm{i}\Omega\frac{1}{\alpha} + \frac{1}{\beta}\right)V(\mathrm{i}\omega) = 0 \tag{35}$$

where the second dimensionless constant is defined as

$$\beta = \omega_n^2 L_i C_p \tag{36}$$

and is the ratio of the mechanical to electrical natural frequencies. Similar to equation (20), this equation can be written in matrix form with the equation of motion of the mechanical system (17) as

$$\begin{bmatrix} \left(1-\Omega^2\right)+2\mathrm{i}\Omega\zeta & -\frac{\theta}{k} \\ -\Omega^2\frac{\alpha\beta\theta}{C_p} & \alpha\left(1-\beta\Omega^2\right)+\mathrm{i}\Omega\beta \end{bmatrix} \begin{Bmatrix} Y(\mathrm{i}\omega) \\ V(\mathrm{i}\omega) \end{Bmatrix} = \begin{Bmatrix} F_0 \\ 0 \end{Bmatrix} \tag{37}$$

Inverting the coefficient matrix, the displacement and voltage in the frequency domain can be obtained as

$$\begin{Bmatrix} Y(\mathrm{i}\omega) \\ V(\mathrm{i}\omega) \end{Bmatrix} = \frac{1}{\Delta_2} \begin{bmatrix} \alpha\left(1-\beta\Omega^2\right)+\mathrm{i}\Omega\beta & \frac{\theta}{k} \\ \Omega^2\frac{\alpha\beta\theta}{C_p} & \left(1-\Omega^2\right)+2\mathrm{i}\Omega\zeta \end{bmatrix} \begin{Bmatrix} F_0 \\ 0 \end{Bmatrix} = \begin{Bmatrix} \left(\alpha\left(1-\beta\Omega^2\right)+\mathrm{i}\Omega\beta\right)F_0/\Delta_2(\mathrm{i}\omega) \\ \Omega^2\frac{\alpha\beta\theta}{C_p}F_0/\Delta_2(\mathrm{i}\omega) \end{Bmatrix} \tag{38}$$

where the determinant of the coefficient matrix is

$$\Delta_2(\mathrm{i}\Omega) = (\mathrm{i}\Omega)^4\beta\,\alpha + (2\,\zeta\,\beta\,\alpha+\beta)\,(\mathrm{i}\Omega)^3 + \left(\beta\,\alpha+\alpha+2\,\zeta\,\beta+\kappa^2\beta\,\alpha\right)(\mathrm{i}\Omega)^2 + (\beta+2\,\zeta\,\alpha)\,(\mathrm{i}\Omega)+\alpha \tag{39}$$

We first consider the case of deterministic excitation. Like the previous case, both the response quantities are expressed in non-dimensional forms. For the displacement response one has

$$\widehat{Y}(\mathrm{i}\Omega) = \frac{Y(\mathrm{i}\Omega)}{Y_0} = \frac{\alpha\left(1-\beta\Omega^2\right)+\mathrm{i}\Omega\beta}{\Delta_2(\mathrm{i}\Omega)} \tag{40}$$

As before, the voltage at $\Omega = 1$ when the damping is zero is considered to be used for the normalisation

$$V_0 = V(\mathrm{i}\Omega)|_{\{\Omega=1,\zeta=0\}} = \frac{\frac{\alpha\beta\theta}{C_p}F_0}{-\alpha\beta\kappa^2} \tag{41}$$

Using this, we obtain the non-dimensional voltage response as

$$\widehat{V}(\mathrm{i}\Omega) = \frac{V(\mathrm{i}\Omega)}{V_0} = \alpha\beta\kappa^2\frac{(\mathrm{i}\Omega)^2}{\Delta_2(\mathrm{i}\Omega)} \tag{42}$$

The main interests are the variation of the dynamic response of the harvester and harvested power as a function of the free stream velocity. In Fig. 5, the non-dimensional displacement amplitude of the harvester given by equation (26) is plotted as function of the non-dimensional free-stream velocity u. The

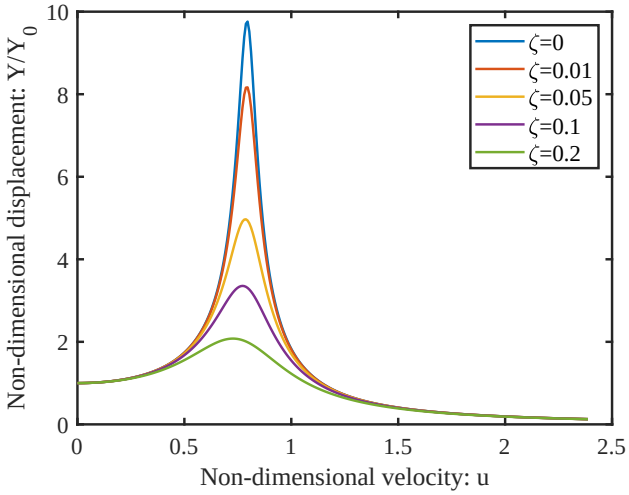

Fig. 5. The non-dimensional displacement amplitude of a harvester with an inductor as a function of the non-dimensional free stream velocity for five selected values of damping factors.

non-dimensional harvested power given by equation (30) is plotted as function of the non-dimensional free-stream velocity u in Fig. 6. For both quantities, five values of the damping factors of energy harvesters

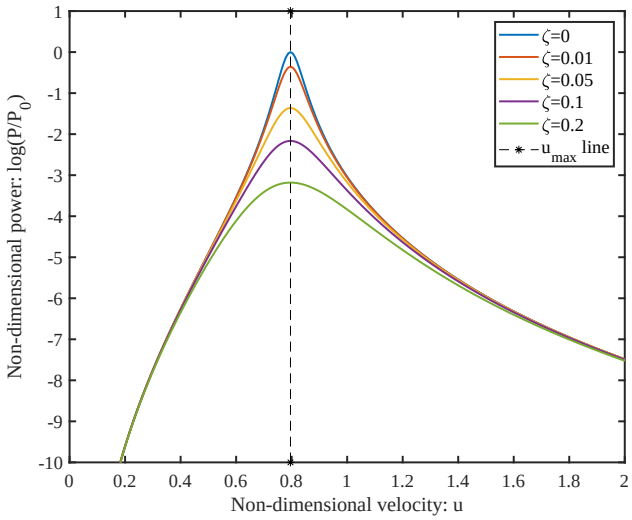

Fig. 6. The non-dimensional power of a harvester with an inductor as a function of the non-dimensional free stream velocity for five selected values of damping factors.

have been considered. As expected, less damping in the harvester leads to more harvested power from the vortex induced vibration. For lightly damped systems, the harvested power peaks about $\Omega \approx 1$. A detailed optimisation analysis shows that the optimal value of the non-dimensional frequency for the maximum power is given by

$$\Omega_{\max}^2 \approx \frac{\left(\left(-3\,\beta^2+\beta\right)\kappa^2+\beta^2-2\,\beta+1\right)\alpha^2+\beta^2}{\left(\left(-4\,\beta^2+2\,\beta\right)\kappa^2+\beta^2-2\,\beta+1\right)\alpha^2+\beta^2} \tag{43}$$

The non-dimensional velocity for the maximum harvested power is, therefore, a function of the Strouhal number, the dimensionless time constant, electromechanical coupling coefficient and the dimensionless inductor constant. The value of $u_{\max}$ is shown in Fig. 6 and we can observe that it matches with the flow velocity for which the harvested power is maximum for all the damping values.

4. The random process model

We consider that the excitation force due to vortex shedding $f_L(t)$ is a random process [43, 44] as this is time-varying function. A wide range of random processes can be used to model uncertainties around the flow field which contribute towards external excitation to the piezoelectric vibration energy harvester. We consider a bounded, weakly stationary, narrowband random process $\eta(t)$ such that the forcing function is given by

$$f_L(t) = \frac{1}{2}\rho U^2 D C_L \eta(t) \tag{44}$$

where

$$\eta(t) = \cos\left(\nu t + \sigma W(t) + \gamma\right) \tag{45}$$

Here ν is the central vortex shedding frequency, $W(t)$ is the standard Wiener process [45] and σ is the strength of the random process. The constant γ is a uniform random variable between 0 to 2π describing the phase of the vortex induced excitation. Zhu [46] used the function in (45) to model randomness in the flow velocity to investigate stability of flow-induced vibration. Cai and Wu [47] conducted a detailed study of a stochastic function similar to (45) in the context of bounded stochastic processes. In the special case when both σ and γ is zero, the excitation function in (44) becomes the standard deterministic excitation as considered in Eq. (14). Therefore, comparing both the equations, the parameter ν in (45) would correspond to the frequency ω_s in the deterministic counterpart. The physical justification behind the choice of the function in (45) is that the random flow is effectively generated by a random perturbation from a mean flow given by (44).

A standard Wiener process $W(t)$ (often called Brownian motion) is a continuous-time stochastic process for $t >= 0$ with $W(0) = 0$ and such that the increment $W(t) - W(s)$ is Gaussian with mean 0 and variance

$t - s$ for any $0 <= s < t$, and increments for nonoverlapping time intervals are independent. Therefore,

$$W(0) = 0 \tag{46}$$

$$W(t) - W(s) \sim \left(\sqrt{t-s}\,\right) N(0,1) \quad 0 \leq s \leq t \tag{47}$$

The probability density function of γ is given by

$$p_\gamma = \frac{1}{2\pi} \tag{48}$$

In Fig. 7 five representative samples of the standard Wiener process and forcing random process $\eta(t)$ have been shown. The samples are generated using the Monte Carlo simulation approach (see for example

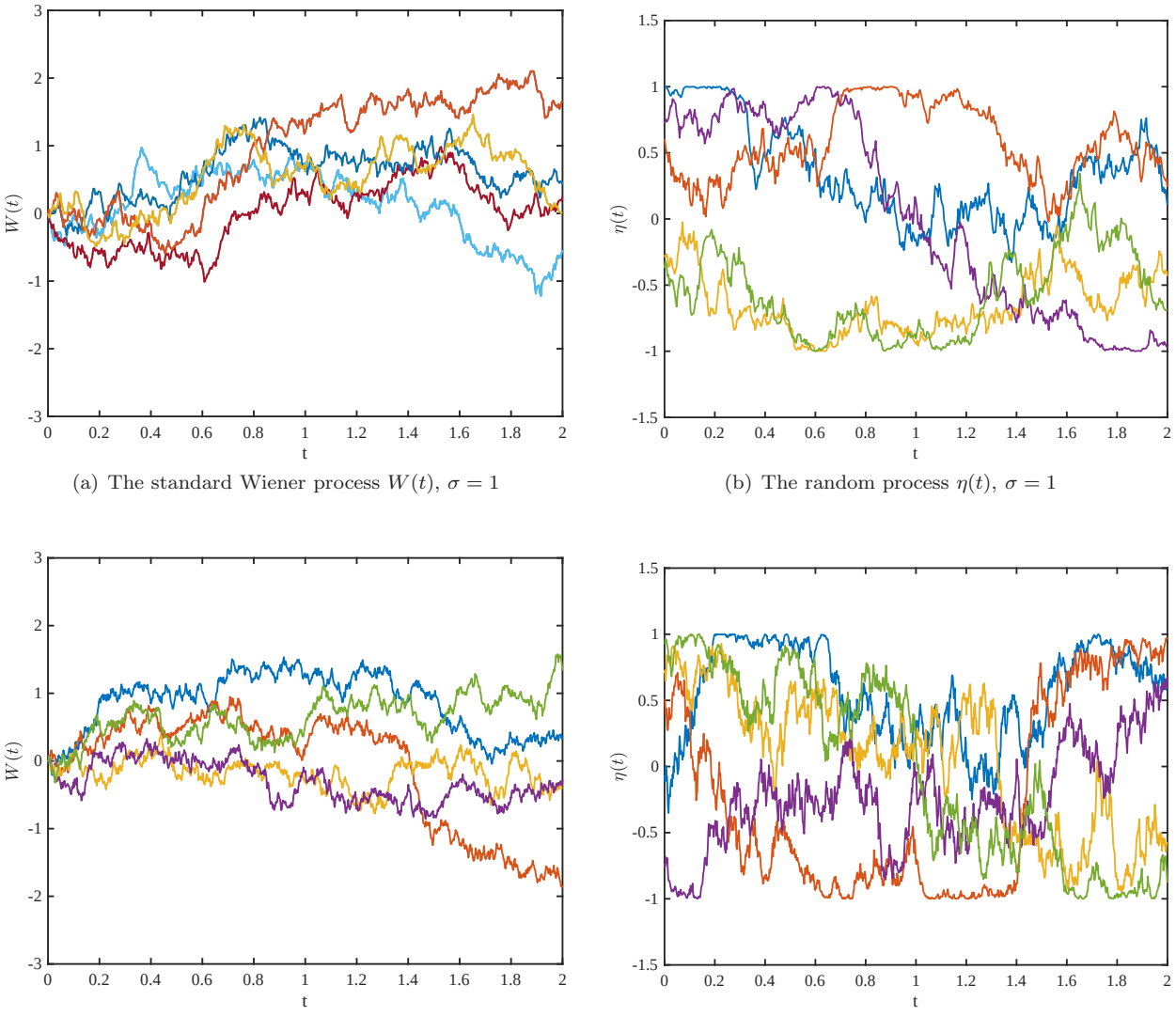

(a) The standard Wiener process $W(t)$, $\sigma = 1$

(b) The random process $\eta(t)$, $\sigma = 1$

(c) The standard Wiener process $W(t)$, $\sigma = 1.5$

(d) The random process $\eta(t)$ $\sigma = 1.5$

Fig. 7. Samples of the standard Wiener process $W(t)$ and the forcing random process $\eta(t)$. For the numerical results 1001 points have been used in the Monte Carlo simulation with $\nu = 1$ and two different values of σ. Five samples taken at random have been shown for t up to 2 seconds.

[48]). Compared to the deterministic case with perfect harmonic excitations considered in the previous section, the forcing function $\eta(t)$ is randomly perturbed from the baseline cosine function. For the numerical results, 1001 points have been used in the Monte Carlo simulation with $\nu = 1$ and two different values of σ have been used. Although the random function is bounded between ± 1, significant variabilities can be observed at a given point in time. The impact of this random perturbation on the energy generation will be quantified in the paper.

Since $\eta(t)$ is a weakly stationary random process, its autocorrelation function depends only on the difference in the time instants

$$\mathrm{E}\left[\eta(\tau_1)\eta(\tau_2)\right] = R_{\eta\eta}(\tau_1 - \tau_2) \tag{49}$$

After some algebra, the autocorrelation function of $\eta(t)$ can be derived as

$$R_{\eta\eta}(\tau) = \frac{1}{2}\cos(\nu\tau)e^{-\frac{1}{2}\sigma^2|\tau|} \tag{50}$$

where $\tau = \tau_1 - \tau_2$ denotes the difference between two time instants. The power spectral density of the random process can be obtained using the Fourier transform of the autocorrelation function as

$$\Phi_{\eta\eta}(\omega) = \int_{-\infty}^{\infty} R_{\eta\eta}(\tau)e^{-\mathrm{i}\omega\tau}\mathrm{d}\tau \tag{51}$$

Substituting the autocorrelation function from (50) into the above equation and after some algebraic simplification the power spectral density [46, 47] is given by

$$\Phi_{\eta\eta}(\omega) = \frac{\sigma^2\left(\omega^2 + \nu^2 + \sigma^4/4\right)}{2\left[(\omega-\nu)^2 + \sigma^4/4\right]\left[(\omega+\nu)^2 + \sigma^4/4\right]} \tag{52}$$

It is convenient to express this in terms of the non-dimensional frequency Ω as

$$\Phi_{\eta\eta}(\Omega) = \frac{\widehat{\sigma}^2\left(\Omega^2 + \widehat{\nu}^2 + \widehat{\sigma}^4/4\right)}{2\omega_n\left[(\Omega-\widehat{\nu})^2 + \widehat{\sigma}^4/4\right]\left[(\Omega+\widehat{\nu})^2 + \widehat{\sigma}^4/4\right]} \tag{53}$$

where the non-dimensional central frequency and the normalised standard deviation are given by

$$\widehat{\nu} = \frac{\nu}{\omega_n} \quad \text{and} \quad \widehat{\sigma}^2 = \frac{\sigma^2}{\omega_n} \tag{54}$$

The power spectral density function of $\Phi_{\eta\eta}(\Omega)$ in equation (53) is plotted in Fig. 8 for two representative values of the normalised standard deviation and four representative values of the non-dimensional central frequency. As expected, the power spectral density function is symmetric about the y-axis. Some key

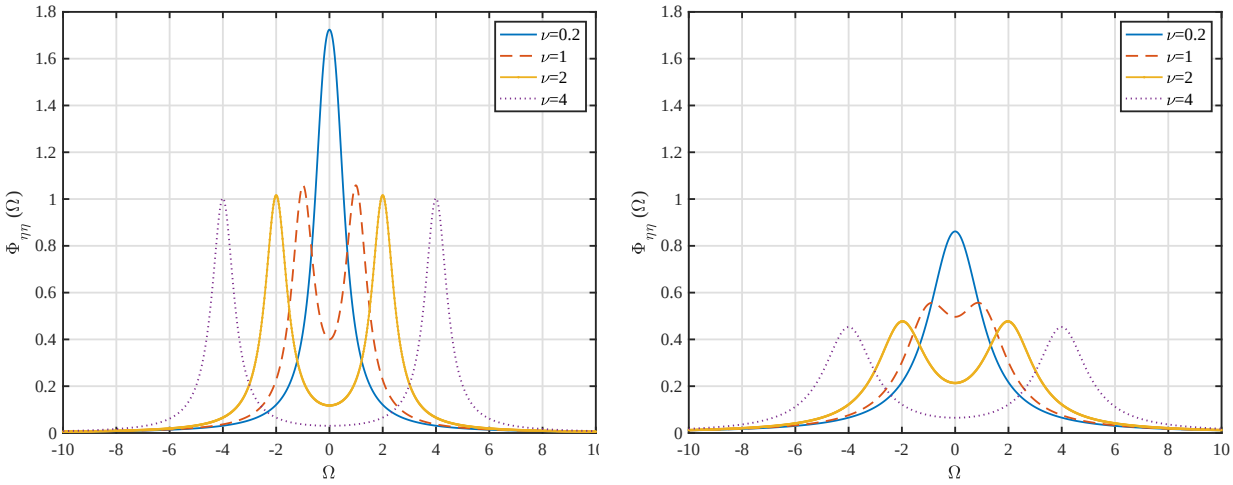

(a) Power spectral density $\Phi_{\eta\eta}(\Omega)$ for $\widehat{\sigma} = 1$

(b) Power spectral density $\Phi_{\eta\eta}(\Omega)$ for $\widehat{\sigma} = 1.5$

Fig. 8. The power spectral density the forcing random process $\eta(t)$ for four different values of non-dimensional central frequency $\widehat{\nu}$.

observations from these plots are:

- The power spectral density function of the input excitation has a peak around the central vortex shedding frequency.

- The sharpness of the peak is governed by the standard deviation of the standard Wiener process $W(t)$. This quantifies the 'amount' of uncertainty in the excitation force. The lower the standard deviation, the sharper the peaks become around their respective central frequencies. In the limit when $\sigma \to 0$, the power spectral density function approaches a Dirac delta function and the excitation becomes a deterministic harmonic excitation as discussed in the previous section. Conversely, when σ becomes large, the spectral density function becomes flattered and in the limit, it approaches to a broad-band excitation (similar to white noise).

This random function physically models the uncertainty of the fluid flow exiting the harvester. The central vortex shedding frequency ν in equation (45) is considered as a free parameter for the sake of generality. This should be as close to the natural frequency of the harvester as possible. Therefore, without any loss of generality, we will consider $\widehat{\nu} = 1$ in our numerical calculations. Previous works which considered random excitations only focused on broadband excitations [41, 49, 50]. Next, we outline methods to derive expressions for dynamic response of the harvester subjected to random excitations with the narrowband power spectral density as shown in Fig. 8.

5. Dynamic response of the energy harvester due to random flow

Mechanical systems driven by random excitations have been discussed by Lin [45], Nigam [51], Bolotin [52], Roberts and Spanos [53] and Newland [54] within the scope of random vibration theory. To obtain the samples of the random response quantities such as the displacement of the mass $y(t)$ and the voltage $v(t)$, one needs to solve the coupled stochastic differential equations (10) and (11) or (10) and (34). However, analytical results developed within the theory of random vibration allows us to bypass numerical solutions because we are interested in the average values of the output random processes. Here we extend the available results to the energy harvester subjected to vortex induced vibration.

In this paper, we are interested in the average harvested power given by

$$\mathrm{E}\left[P(t)\right] = \mathrm{E}\left[\frac{v^2(t)}{R_l}\right] = \frac{\mathrm{E}\left[v^2(t)\right]}{R_l} \tag{55}$$

For a damped linear system of the form $V(\omega) = H(\omega)\widehat{\eta}(\omega)$, it can be shown that [45, 51] the spectral density of V is related to the spectral density of η by

$$\Phi_{VV}(\omega) = |H(\omega)|^2 \Phi_{\eta\eta}(\omega) \tag{56}$$

Here $\widehat{\eta}(\omega)$ is the Fourier transform of $\eta(t)$ and $\Phi_{\eta\eta}(\omega)$ is the power spectral density of the random process $\eta(t)$. For large values of t, taking the limit, we obtain

$$\mathrm{E}\left[v^2(t)\right] = R_{vv}(0) = \int_{-\infty}^{\infty} |H(\omega)|^2 \Phi_{\eta\eta}(\omega)\, \mathrm{d}\omega \tag{57}$$

This expression will be used to obtain the average power for the two cases considered.

The calculation of the integral on the right-hand side of equation (57) in general requires the calculation of integrals of the following form

$$I_n = \int_{-\infty}^{\infty} \frac{\Xi_n(\omega)\, \mathrm{d}\omega}{\Lambda_n(\omega)\Lambda_n^*(\omega)} \tag{58}$$

where the polynomials have the form

$$\Xi_n(\omega) = b_{n-1}\omega^{2n-2} + b_{n-2}\omega^{2n-4} + \cdots + b_0 \tag{59}$$

$$\Lambda_n(\omega) = a_n(\mathrm{i}\omega)^n + a_{n-1}(\mathrm{i}\omega)^{n-1} + \cdots + a_0 \tag{60}$$

The evaluation of the integral in equation (58) requires contour integration techniques. Following Roberts and Spanos [53] this integral can be evaluated as

$$I_n = \frac{\pi}{a_n} \frac{\det \mathbf{N}_n}{\det \mathbf{D}_n}. \tag{61}$$

Here the $n \times n$ matrices are defined as

$$\mathbf{N}_n = \begin{bmatrix} b_{n-1} & b_{n-2} & & \cdots & & & b_0 \\ -a_n & a_{n-2} & -a_{n-4} & a_{n-6} & \cdots & 0 & \cdots \\ 0 & -a_{n-1} & a_{n-3} & -a_{n-5} & \cdots & 0 & \cdots \\ 0 & a_n & -a_{n-2} & a_{n-4} & \cdots & 0 & \cdots \\ 0 & \cdots & & & \cdots & 0 & \cdots \\ 0 & 0 & & & \cdots & -a_2 & a_0 \end{bmatrix} \tag{62}$$

and

$$\mathbf{D}_n = \begin{bmatrix} a_{n-1} & -a_{n-3} & a_{n-5} & -a_{n-7} & & & \\ -a_n & a_{n-2} & -a_{n-4} & a_{n-6} & \cdots & 0 & \cdots \\ 0 & -a_{n-1} & a_{n-3} & -a_{n-5} & \cdots & 0 & \cdots \\ 0 & a_n & -a_{n-2} & a_{n-4} & \cdots & 0 & \cdots \\ 0 & \cdots & & & \cdots & 0 & \cdots \\ 0 & 0 & & & \cdots & -a_2 & a_0 \end{bmatrix}. \tag{63}$$

These expressions will be used for the two cases considered.

6. The quantification of harvested power

6.1. Mean power for systems without an inductor

The main focus in this section is to obtain the mean of the non-dimensional harvested power given by equation (30) when the flow is random in nature. From equation (29) and using equation (45) we obtain the non-dimensional voltage in the frequency domain as

$$V(\mathrm{i}\Omega) = \underbrace{\alpha\kappa^2 \frac{\mathrm{i}\Omega}{\Delta_1(\mathrm{i}\Omega)}}_{H(\Omega)} \widehat{\eta}(\Omega) \tag{64}$$

Here $\widehat{\eta}(\Omega)$ is the Fourier transform of $\eta(t)$ in equation (45) expressed in terms of the non-dimensional frequency parameter Ω. Its power spectral density is given by equation (53). Setting the numerator to zero we note that there are four roots

$$\Omega_j (j = 1, \cdots, 4) = \pm\widehat{\nu} \pm \mathrm{i}\sigma^2/2 \tag{65}$$

$$\text{or} \quad \mathrm{i}\Omega_j (j = 1, \cdots, 4) = \mp\sigma^2/2 \mp \mathrm{i}\widehat{\nu} \tag{66}$$

Therefore, the denominator can be factorised as

$$2\omega_n(\alpha_1 + \mathrm{i}\Omega)(\alpha_2 + \mathrm{i}\Omega)(\alpha_1 - \mathrm{i}\Omega)(\alpha_2 - \mathrm{i}\Omega) \tag{67}$$

where

$$\alpha_1 = \sigma^2/2 - \mathrm{i}\widehat{\nu} \quad \text{and} \quad \alpha_2 = \sigma^2/2 - \mathrm{i}\widehat{\nu} = \alpha_1^* \tag{68}$$

Using these, after some algebra, the power spectra density in (53) can be expressed as

$$\Phi_{\eta\eta}(\Omega) = \frac{\widehat{\sigma}^2 \left(\Omega^2 + \widehat{c}^2\right)}{2\omega_n \left\{F_\eta(\mathrm{i}\Omega) F_\eta^*(\mathrm{i}\Omega)\right\}} \tag{69}$$

where

$$\widehat{c}^2 = \widehat{\nu}^2 + \widehat{\sigma}^4/4 \tag{70}$$

and

$$F_\eta(\mathrm{i}\Omega) = \widehat{c}^2 + \widehat{\sigma}^2(\mathrm{i}\Omega) + (\mathrm{i}\Omega)^2 \tag{71}$$

The expression of the non-dimensional power is given by equation (30). We are interested in obtaining the mean of this quantity

$$\mathrm{E}\left[\widehat{P}\right] = \mathrm{E}\left[\left|\widehat{V}(\mathrm{i}\Omega)\right|^2\right] \tag{72}$$

Employing a change of variable $\omega = \Omega\omega_n$ and using equation (72) we have

$$\mathrm{E}\left[\widehat{P}\right] = \omega_n \int_{-\infty}^{\infty} |H(\Omega)|^2 \Phi_{\eta\eta}(\Omega)\, \mathrm{d}\Omega \tag{73}$$

Using the expression of $H(\Omega)$ from equation (64) and $\Phi_{\eta\eta}(\Omega)$ from equation (69), the non-dimensional mean power can be obtained by

$$\mathrm{E}\left[\widehat{P}\right] = \omega_n \int_{-\infty}^{\infty} (\alpha\kappa^2)^2 \frac{\Omega^2}{\Delta_1(\mathrm{i}\Omega)\Delta_1^*(\mathrm{i}\Omega)} \frac{\widehat{\sigma}^2\left(\Omega^2 + \widehat{c}^2\right)}{2\omega_n\left\{F_\eta(\mathrm{i}\Omega)F_\eta^*(\mathrm{i}\Omega)\right\}}\, \mathrm{d}\Omega \tag{74}$$

$$= \frac{1}{2}(\alpha\kappa^2\widehat{\sigma})^2 \int_{-\infty}^{\infty} \frac{\Omega^2\left(\Omega^2 + \widehat{c}^2\right)}{G_1(\mathrm{i}\Omega)G_1^*(\mathrm{i}\Omega)}\, \mathrm{d}\Omega \tag{75}$$

Here the denominator function

$$\begin{aligned} G_1(\mathrm{i}\Omega) &= \Delta_1(\mathrm{i}\Omega)F_\eta(\mathrm{i}\Omega) \\ &= \left\{(\mathrm{i}\Omega)^3\alpha + (2\,\zeta\,\alpha + 1)\,(\mathrm{i}\Omega)^2 + \left(\alpha + \kappa^2\alpha + 2\,\zeta\right)(\mathrm{i}\Omega) + 1\right\}\left\{\widehat{c}^2 + \widehat{\sigma}^2(\mathrm{i}\Omega) + (\mathrm{i}\Omega)^2\right\} \end{aligned} \tag{76}$$

is a fifth order polynomial in $\mathrm{i}\Omega$. This can be expressed in the form of (60) with

$$\begin{aligned} a_0 &= \widehat{c}^2 \\ a_1 &= \alpha\,\widehat{c}^2\kappa^2 + 2\,\zeta\,\widehat{c}^2 + \alpha\,\widehat{c}^2 + \widehat{\sigma} \\ a_2 &= 2\,\zeta\,\alpha\,\widehat{c}^2 + \alpha\,\kappa^2\widehat{\sigma} + 2\,\zeta\,\widehat{\sigma} + \alpha\,\widehat{\sigma} + \widehat{c}^2 + 1 \\ a_3 &= 2\,\zeta\,\alpha\,\widehat{\sigma} + \alpha\,\widehat{c}^2 + \alpha\,\kappa^2 + 2\,\zeta + \alpha + \widehat{\sigma} \\ a_4 &= 2\,\zeta\,\alpha + \alpha\,\widehat{\sigma} + 1 \\ a_5 &= \alpha \end{aligned} \tag{77}$$

From equation (75), the average non-dimensional harvested power from vortex induced vibration arising from randomly fluctuating flow can be expressed as

$$\mathrm{E}\left[\widehat{P}\right] = \frac{1}{2}(\alpha\kappa^2\widehat{\sigma})^2 I^{(1)} \tag{78}$$

where

$$I^{(1)} = \int_{-\infty}^{\infty} \frac{\Omega^4 + \widehat{c}^2\Omega^2}{G_1(\mathrm{i}\Omega)G_1^*(\mathrm{i}\Omega)}\, \mathrm{d}\Omega \tag{79}$$

Comparing $I^{(1)}$ with the general integral in equation (58) we have

$$n = 5, b_1 = \widehat{c}^2, b_2 = 1, b_0 = b_3 = b_4 = 0 \tag{80}$$

Now using equation (61), the integral can be evaluated as

$$\begin{aligned} I^{(1)} &= \frac{\pi}{\alpha} \frac{\det\begin{bmatrix} 0 & 0 & 1 & \widehat{c}^2 & 0 \\ -\alpha & a_3 & -a_1 & 0 & 0 \\ 0 & -a_4 & a_2 & \widehat{c}^2 & 0 \\ 0 & \alpha & -a_3 & a_1 & 0 \\ 0 & 0 & a_4 & -a_2 & \widehat{c}^2 \end{bmatrix}}{\det\begin{bmatrix} a_4 & -a_2 & \widehat{c}^2 & 0 & 0 \\ -\alpha & a_3 & -a_1 & 0 & 0 \\ 0 & -a_4 & a_2 & \widehat{c}^2 & 0 \\ 0 & \alpha & -a_3 & a_1 & 0 \\ 0 & 0 & a_4 & -a_2 & \widehat{c}^2 \end{bmatrix}} \\ &= \pi \frac{\left(-\alpha\,a_2 + a_3a_4 + \alpha\right)\widehat{c}^2 + a_1a_4}{\alpha^2\widehat{c}^4 + \left(-\alpha\,a_2a_3 + {a_3}^2a_4\right)\widehat{c}^2 - \alpha\,a_1{a_2}^2 - {a_1}^2{a_4}^2 + a_1a_2a_3a_4} \end{aligned} \tag{81}$$

Combining this with equation (78) we finally obtain the average harvested power as

$$\mathrm{E}\left[\widehat{P}\right] = \frac{\pi}{2}(\alpha\kappa^2\widehat{\sigma})^2 \frac{(-\alpha\, a_2 + a_3a_4 + \alpha)\,\widehat{c}^2 + a_1a_4}{\alpha^2\widehat{c}^4 + (-\alpha\, a_2a_3 + {a_3}^2a_4)\,\widehat{c}^2 - \alpha\, a_1{a_2}^2 - {a_1}^2{a_4}^2 + a_1a_2a_3a_4} \tag{82}$$

where the constants $a_j, j = 1, \cdots, 4$ are defined in (77). The mean of non-dimensional harvested power obtained form this closed-form equation is plotted in Fig. 9 as functions of α, ζ and κ. Since α and κ^2

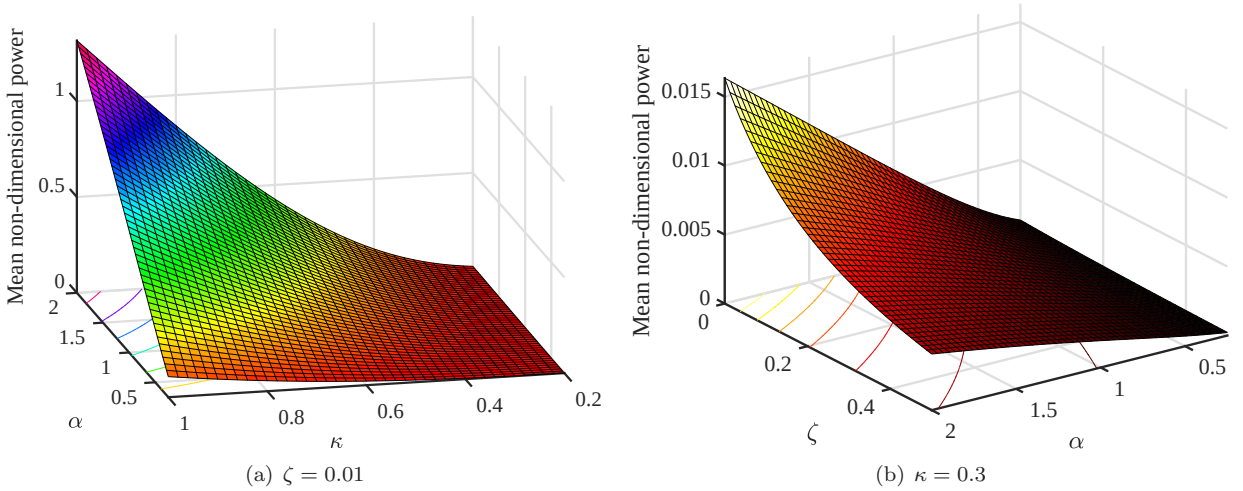

(a) $\zeta = 0.01$ (b) $\kappa = 0.3$

Fig. 9. The mean of non-dimensional harvested power from the vortex induced vibration as functions of α, ζ and κ. The normalised random field parameters are $\widehat{\sigma} = 1$ and $\widehat{\nu} = 1$.

are positive, the average harvested power is monotonically decreasing with damping ratio ζ. Thus the mechanical damping in the harvester should be minimised. For fixed α and ζ the average harvested power is monotonically increasing with the coupling coefficient κ^2, and hence the electromechanical coupling should be as large as possible.Additionally, we observe that for fixed κ and ζ the average harvested power is monotonically increasing with the coupling coefficient α.

6.2. Mean power for systems with an inductor

From equation (42) and using equation (45) we obtain the non-dimensional voltage in the frequency domain as

$$V(\mathrm{i}\Omega) = \underbrace{\frac{V(\mathrm{i}\Omega)}{V_0} = \alpha\beta\kappa^2 \frac{(\mathrm{i}\Omega)^2}{\Delta_2(\mathrm{i}\Omega)}}_{H(\Omega)} \widehat{\eta}(\Omega) \tag{83}$$

Using the above $H(\Omega)$ and $\Phi_{\eta\eta}(\Omega)$ from equation (69), the non-dimensional mean power can be obtained by

$$\mathrm{E}\left[\widehat{P}\right] = \omega_n \int_{-\infty}^{\infty} (\alpha\beta\kappa^2)^2 \frac{\Omega^4}{\Delta_2(\mathrm{i}\Omega)\Delta_2^*(\mathrm{i}\Omega)} \frac{\widehat{\sigma}^2\left(\Omega^2 + \widehat{c}^2\right)}{2\omega_n\left\{F_\eta(\mathrm{i}\Omega)F_\eta^*(\mathrm{i}\Omega)\right\}}\,\mathrm{d}\Omega \tag{84}$$

$$= \frac{1}{2}(\alpha\beta\kappa^2\widehat{\sigma})^2 \int_{-\infty}^{\infty} \frac{\Omega^4\left(\Omega^2 + \widehat{c}^2\right)}{G_2(\mathrm{i}\Omega)G_2^*(\mathrm{i}\Omega)}\,\mathrm{d}\Omega \tag{85}$$

Here the denominator function

$$G_2(\mathrm{i}\Omega) = \Delta_2(\mathrm{i}\Omega)F_\eta(\mathrm{i}\Omega) = a_n(\mathrm{i}\omega)^n + a_{n-1}(\mathrm{i}\omega)^{n-1} + \cdots + a_0, \quad \text{and} \quad n = 6 \tag{86}$$

is a sixth order polynomial in $\mathrm{i}\Omega$. The coefficients can be obtained as

$$\begin{aligned}
a_0 &= \alpha\,\widehat{c}^2,\\
a_1 &= 2\,\alpha\,\widehat{c}^2\zeta_n + \beta\,\widehat{c}^2 + \alpha\,\sigma,\\
a_2 &= \alpha\,\beta\,\widehat{c}^2\kappa^2 + \alpha\,\beta\,\widehat{c}^2 + 2\,\beta\,\widehat{c}^2\zeta_n + \alpha\,\widehat{c}^2 + 2\,\alpha\,\sigma\,\zeta_n + \beta\,\sigma + \alpha,\\
a_3 &= 2\,\alpha\,\beta\,\widehat{c}^2\zeta_n + \alpha\,\beta\,\kappa^2\sigma + \alpha\,\beta\,\sigma + \beta\,\widehat{c}^2 + 2\,\beta\,\sigma\,\zeta_n + \alpha\,\sigma + 2\,\alpha\,\zeta_n + \beta,\\
a_4 &= \alpha\,\beta\,\widehat{c}^2 + \alpha\,\beta\,\kappa^2 + 2\,\alpha\,\beta\,\sigma\,\zeta_n + \alpha\,\beta + \beta\,\sigma + 2\,\beta\,\zeta_n + \alpha,\\
a_5 &= \alpha\,\beta\,\sigma + 2\,\alpha\,\beta\,\zeta_n + \beta,\\
a_6 &= \alpha\,\beta
\end{aligned} \tag{87}$$

From equation (85), the average non-dimensional harvested power from vortex induced vibration arising from randomly fluctuating flow can be expressed as

$$\mathrm{E}\left[\widehat{P}\right] = \frac{1}{2}(\alpha\beta\kappa^2\widehat{\sigma})^2 I^{(2)} \tag{88}$$

where

$$I^{(2)} = \int_{-\infty}^{\infty} \frac{\Omega^6 + \widehat{c}^2\Omega^4}{G_2(\mathrm{i}\Omega)G_2^*(\mathrm{i}\Omega)}\,\mathrm{d}\Omega \tag{89}$$

Comparing $I^{(2)}$ with the general integral in equation (58) we have

$$n = 6, b_2 = \widehat{c}^2, b_3 = 1, b_0 = b_1 = b_3 = b_4 = 0 \tag{90}$$

Now using equation (61), the integral can be evaluated as

$$\begin{aligned}
I^{(2)} &= \frac{\pi}{\alpha\beta}\frac{\det\begin{bmatrix} 0 & 0 & 1 & \widehat{c}^2 & 0 & 0\\ -\alpha\,\beta & a_4 & -a_2 & \alpha\,\widehat{c}^2 & 0 & 0\\ 0 & -a_5 & a_3 & -a_1 & 0 & 0\\ 0 & \alpha\,\beta & -a_4 & a_2 & -\alpha\,\widehat{c}^2 & 0\\ 0 & 0 & a_5 & -a_3 & a_1 & 0\\ 0 & 0 & -\alpha\,\beta & a_4 & -a_2 & \alpha\,\widehat{c}^2 \end{bmatrix}}{\det\begin{bmatrix} a_5 & -a_3 & a_1 & 0 & 0 & 0\\ -\alpha\,\beta & a_4 & -a_2 & \alpha\,\widehat{c}^2 & 0 & 0\\ 0 & -a_5 & a_3 & -a_1 & 0 & 0\\ 0 & \alpha\,\beta & -a_4 & a_2 & -\alpha\,\widehat{c}^2 & 0\\ 0 & 0 & a_5 & -a_3 & a_1 & 0\\ 0 & 0 & -\alpha\,\beta & a_4 & -a_2 & \alpha\,\widehat{c}^2 \end{bmatrix}}\\
&= \pi\frac{\alpha\,\widehat{c}^4{a_5}^2 + (\alpha\,\beta\,a_1a_3 + \alpha\,a_3a_5 - a_1a_4a_5)\,\widehat{c}^2 + \alpha\,\beta\,{a_1}^2 - a_1a_2a_5}{\alpha^2\widehat{c}^4{a_5}^3 + \left(3\,\alpha^2\beta\,a_1a_3a_5 - \alpha^2\beta\,{a_3}^3 - 2\,\alpha\,a_1a_4{a_5}^2 - \alpha\,a_2a_3{a_5}^2 + \alpha\,{a_3}^2a_4a_5\right)\widehat{c}^2 + \alpha^2\beta^2{a_1}^3}\\
&\qquad -2\,\alpha\,\beta\,{a_1}^2a_2a_5 - \alpha\,\beta\,{a_1}^2a_3a_4 + \alpha\,\beta\,a_1a_2{a_3}^2 + {a_1}^2{a_4}^2a_5 + a_1{a_2}^2{a_5}^2 - a_1a_2a_3a_4a_5
\end{aligned} \tag{91}$$

Substituting this in equation (88), the average harvested power can be obtained using a closed-form expression. The constants $a_j, j = 1, \cdots, 5$ are defined in equation (87). The mean of non-dimensional harvested power obtained form this closed-form equation is plotted in Fig. 10 as functions of α, ζ and κ. We observe that the average harvested power is monotonically decreasing with damping ratio ζ and monotonically increasing with the time constant α. Thus the mechanical damping in the harvester should be minimised. For a fixed α, β and ζ the average harvested power is monotonically increasing with the coupling coefficient κ^2, and hence the electromechanical coupling should be as large as possible. The mean of non-dimensional harvested power obtained form this closed-form equation is shown in Fig. 11 as functions of α, β and κ. A key difference is that the variability in the mean power with respect to β is not a monotonically increasing function. There is a certain value for which the power reaches a peak and then it remains fairly constant. To investigate this further, the mean harvested power as a function of β is shown in Fig. 12. This is plotted with the other parameters fixed at $\zeta = 0.01$ and $\kappa = 0.3$. The optimum value occurs at $\beta = 1$, which is shown by the star in Fig. 12.

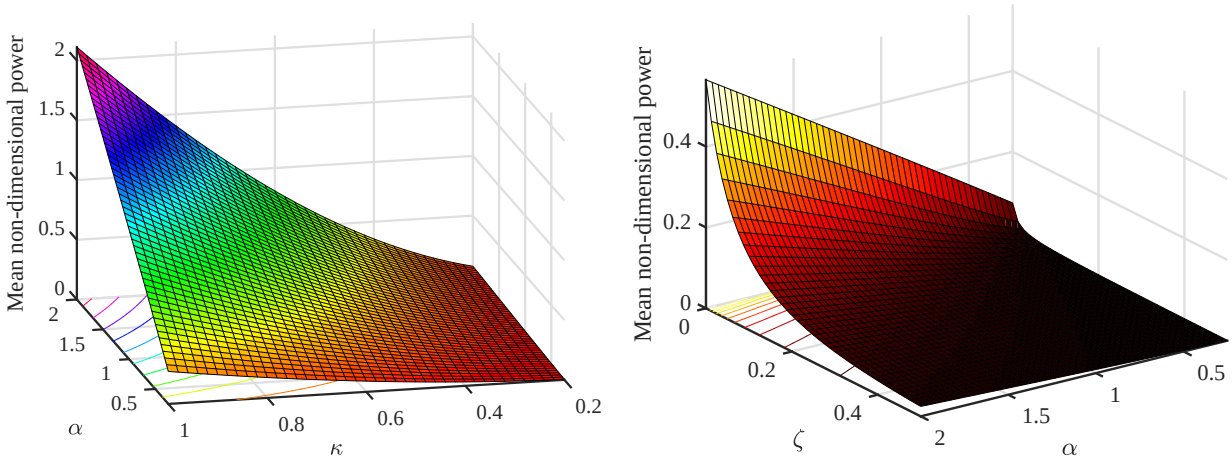

(a) $\zeta = 0.01$, $\beta = 1.0$ (b) $\kappa = 0.3$, $\beta = 1.0$

Fig. 10. The mean of non-dimensional harvested power from the vortex induced vibration as functions of α, ζ and κ. The value of the inductor constant is fixed at $\beta = 1.0$. The normalised random field parameters are $\widehat{\sigma} = 1$ and $\widehat{\nu} = 1$.

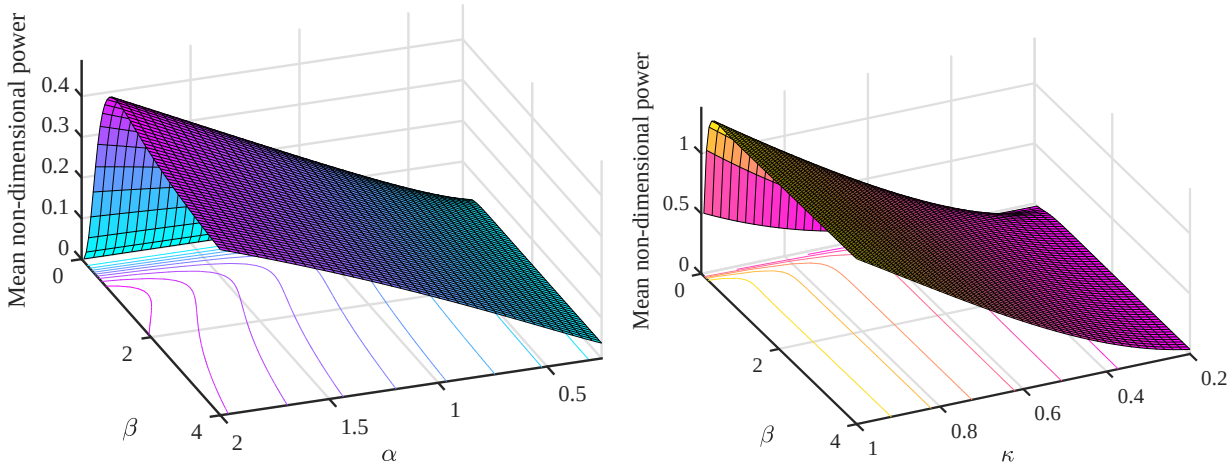

(a) $\zeta = 0.01$, $\kappa = 0.3$ (b) $\zeta = 0.01$, $\alpha = 0.6$

Fig. 11. The mean of non-dimensional harvested power from the vortex induced vibration as functions of α, ζ and κ. The value of the damping factors is fixed at $\zeta = 0.01$. The normalised random field parameters are $\widehat{\sigma} = 1$ and $\widehat{\nu} = 1$.

7. Conclusions

This paper developed the mathematical framework for the analysis of vortex induced vibration energy harvesters incorporating randomness in the flow field. A cantilever beam with PZT layers and a cylindrical bluff body at the tip facing the fluid flow is considered. The excitation to the harvester arises due to vortices originating from the bluff body. A reduced single-degree-of-freedom electromechanical model with fluid-structure interaction is employed. The electromechanical coupling in the model is considered to be arising from unimorph or bimorph PZT configurations. Two cases of energy harvesting circuits, namely, one with an inductor and another without an inductor, have been used. For both the cases, the governing equations are in general represented by coupled second-order ordinary differential equations and they are expressed in terms of non-dimensional coefficients. Additionally, the displacement and voltage response is also transformed into non-dimensional forms for clarity and simplicity. The voltage response of the system has been studied under deterministic flow velocity and optimal velocity for maximum power generation has been obtained analytically. The randomness in the flow velocity is modelled using a narrowband Gaussian random process involving the Wiener process. The power spectral density of the random process has a peak around a central vortex shedding frequency representing the underlying fluid flow with the mean velocity. Monte

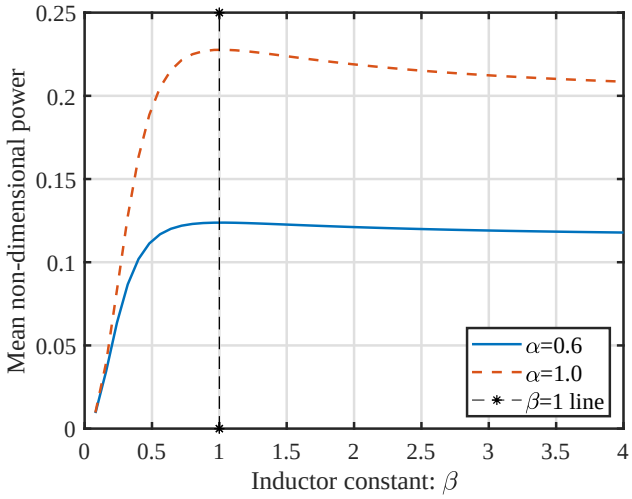

Fig. 12. The mean of non-dimensional harvested power for a harvester with an inductor as a function of β for two values of α with fixed values of $\zeta = 0.01$ and $\kappa = 0.3$. The * corresponds to the optimal value of $\beta(= 1)$ for the maximum mean harvested power.

Carlo simulation results of the samples of the flow velocity field have been presented. Analytical formulations exploiting the theory of random vibration have been proposed to obtain the mean power generated from the energy harvesters with the Wiener process flow velocity. Closed-form formulae for the average normalised harvested power for the energy harvesters without and with an inductor have been derived. Important aspects of this paper include:

- *Simplified single-degree-of-freedom model:* A reduced single-degree-of-freedom model with closed-form expressions for mass, stiffness, damping and electromechanical coupling is given in terms of non-dimensional integrals involving the assumed deformation shape of the cantilever harvester.
- *Non-dimensionalisation of the voltage and power:* A new simple way of expressing the voltage of the system is proposed by normalising it with the maximum voltage arising from the underlying undamped system at the resonance frequency. This, in turn, simplified the stochastic analysis and made the results general in nature.
- *Flow velocity for maximum power:* For the case of deterministic flow, the non-dimensional velocity for maximum harvested power is derived as $u_{\max} = \Omega_{\max}/2\pi S$. Here $\Omega_{\max}$ is obtained using a mathematical optimisation process and is given by (32) or (43) depending on whether the harvesting circuit is without or with an inductor. The constant $\Omega_{\max}$ depends on the electrical parameters only.
- *The random process model:* The random process model describing the flow field is used for the first time in the context of vortex induced vibration energy harvesting. The random process is a function of the Wiener process (Brownian motion) and a uniform distribution. This is a two-parameter narrow-band stationary Gaussian random process with one parameter denoting a central vortex shedding frequency and another parameter quantifying variabilities around that frequency.
- *New closed-form power expressions:* Exact closed-form expressions for average normalised harvested power for energy harvesters without and with an inductor have been derived using contour integration techniques. These formulae eliminate the need for expensive Monte Carlo simulation based direct computations and also provide physical insights.

Results obtained from the derived average power equations have been illustrated numerically for selected parameter values. There are several parameters in the problem and the choice of a particular set qualitatively and quantitatively changes the amount of harvested power. The closed-form expressions derived in the paper provide an easier route for investigating this parametric landscape. The limited parametric analysis is shown here highlights the fact that the average harvested power can be maximised for certain parameter values (β for example). Future work should consider direct practical applications of the analytical expressions. Experimental validations of the closed-form expressions would also be of paramount importance. Potential benefits arising from the design of vortex induced vibration energy harvesters with random flow velocity considerations should be explored further with suitable case studies.

Acknowledgements

SA acknowledges the financial support from the Global Challenges Research Fund, grant number GCRF RIG1029-103. BB and AR acknowledge DST-IUSSTF and SPARC for partial funding of the research through the project grants: IUSSTF/ME /2017400A and MHRD /ME /2018544 respectively.

References

[1] Park G, Rosing T, Todd MD, Farrar CR, Hodgkiss W, Energy Harvesting for Structural Health Monitoring Sensor Networks. *Journal of Infrastructure Systems* 2008; **14**(1):64–79.
[2] Hirt C, Amsden A, Cook J, An arbitrary Lagrangian-Eulerian computing method for all flow speeds. *Journal of Computational Physics* 1974; **14**(3):227 – 253.
[3] Wang X, *Fundamentals of fluid-solid interactions: Analytical and Computational Approaches*. 2008.
[4] Mehmood A, Abdelkefi A, Hajj M, Nayfeh A, Akhtar I, Nuhait A, Piezoelectric energy harvesting from vortex-induced vibrations of circular cylinder. *Journal of Sound and Vibration* 2013; **332**(19):4656–4667.
[5] Cai SG, Ouahsine A, Favier J, Hoarau Y, Moving immersed boundary method. *International Journal for Numerical Methods in Fluids* 2017; **85**(5):288–323.
[6] Soti AK, Thompson MC, Sheridan J, Bhardwaj R, Harnessing electrical power from vortex-induced vibration of a circular cylinder. *Journal of Fluids and Structures* 2017; **70**:360–373.
[7] Yeiser A, A spectral element method for meshes with skinny elements. 2018 .
[8] D. Blevins R, Flow-Induced Vibration. *New York, Van Nostrand Reinhold Co., 1977. 377 p.* 1977; **-1**.
[9] Païdoussis M, J. Price S, de Langre E, Fluid-structure Interactions: Cross-flow-induced Instabilities. *Fluid-Structure Interactions: Cross-Flow-Induced Instabilities* 2010; :1–402.
[10] de Langre E, Frequency lock-in is caused by coupled-mode flutter. *Journal of Fluids and Structures* 2006; **22**:783–791.
[11] Bishop RED, Hassan A, The lift and drag forces on a circular cylinder in a flowing fluid. *Proceedings of the Royal Society of London. Series A. Mathematical and Physical Sciences* 1964; **277**(1368):32–50.
[12] Tamura Y, Matsui G, Wake -oscillator model of vortex-induced oscillation of circular cylinder. *Wind Engineering* (ed. J Cermak), Pergamon, 1980 1085 – 1094, 1085 – 1094.
[13] Skop R, Balasubramanian S, A new twist on an old model for vortex-excited vibrations. *Journal of Fluids and Structures* 1997; **11**(4):395 – 412.
[14] Facchinetti ML, De Langre E, Biolley F, Coupling of structure and wake oscillators in vortex-induced vibrations. *Journal of Fluids and structures* 2004; **19**(2):123–140.
[15] Benaroya H, Wei T, Kuchnicki S, Dong P, Extended Hamilton's principle for fluid-structure interaction. *Proceedings of the Institution of Mechanical Engineers, Part K: Journal of Multi-body Dynamics* 2003; **217**(2):153–170.
[16] Farshidianfar A, Zanganeh H, A modified wake oscillator model for vortex-induced vibration of circular cylinders for a wide range of mass-damping ratio. *Journal of Fluids and Structures* 2010; **26**(3):430 – 441.
[17] Gabbai R, Benaroya H, An overview of modeling and experiments of vortex-induced vibration of circular cylinders. *Journal of Sound and Vibration* 2005; **282**(3):575 – 616.
[18] Pavlovskaia E, Keber M, Postnikov A, Reddington K, Wiercigroch M, Multi-modes approach to modelling of vortex-induced vibration. *International Journal of Non-Linear Mechanics* 2016; **80**:40–51.
[19] Hobeck JD, Inman DJ, Artificial piezoelectric grass for energy harvesting from turbulence-induced vibration. *Smart Materials and Structures* 2012; **21**(10):105024.
[20] Bourguet R, Karniadakis GE, Triantafyllou MS, Vortex-induced vibrations of a long flexible cylinder in shear flow. *Journal of Fluid Mechanics* 2011; **677**:342382.
[21] Antoine GO, de Langre E, Michelin S, Optimal energy harvesting from vortex-induced vibrations of cables. *Proceedings of the Royal Society A-Mathematical, Physical and Engineering Sciences* 2016; **472**(2195).
[22] Wu X, Ge F, Hong Y, A review of recent studies on vortex-induced vibrations of long slender cylinders. *Journal of Fluids and Structures* 2012; **28**:292 – 308.
[23] Dai H, Abdelkefi A, Wang L, Theoretical modeling and nonlinear analysis of piezoelectric energy harvesting from vortex-induced vibrations. *Journal of Intelligent Material Systems and Structures* 2014; **25**.
[24] Hu G, Tse KT, Kwok KCS, Song J, Lyu Y, Aerodynamic modification to a circular cylinder to enhance the piezoelectric wind energy harvesting. *Applied Physics Letters* 2016; **109**(19).
[25] Zhang L, Abdelkefi A, Dai H, Naseer R, Wang L, Design and experimental analysis of broadband energy harvesting from vortex-induced vibrations. *Journal of Sound and Vibration* 2017; **408**:210 – 219.
[26] Zhang L, Dai H, Abdelkefi A, Wang L, Experimental investigation of aerodynamic energy harvester with different interference cylinder cross-sections. *Energy* 2019; **167**:970 – 981.
[27] Li D, Wu Y, Ronch AD, Xiang J, Energy harvesting by means of flow-induced vibrations on aerospace vehicles. *Progress in Aerospace Sciences* 2016; **86**:28 – 62.
[28] Hamlehdar M, Kasaeian A, Safaei MR, Energy harvesting from fluid flow using piezoelectrics: A critical review. *Renewable Energy* 2019; **143**:1826 – 1838.
[29] Daqaq MF, Bibo A, Akhtar I, Alhadidi AH, Panyam M, Caldwell B, Noel J, Micropower Generation Using Cross-Flow Instabilities: A Review of the Literature and Its Implications. *Journal of Vibration and Acoustics-Transactions of the ASME* 2019; **141**.
[30] Zhao L, Yang Y, On the modeling methods of small-scale piezoelectric wind energy harvesting. *Smart Structures and Systems* 2017; **19**(1):67–90.
[31] Abdelkefi A, Aeroelastic energy harvesting: A review. *International Journal of Engineering Science* 2016; **100**:112–135.
[32] Petrini F, Gkoumas K, Piezoelectric energy harvesting from vortex shedding and galloping induced vibrations inside HVAC ducts. *Energy and Buildings* 2018; **158**:371–383.
[33] Shan X, Song R, Liu B, Xie T, Novel energy harvesting: A macro fiber composite piezoelectric energy harvester in the water vortex. *Ceramics International* 2015; **41**:S763 – S767, the 9th Asian Meeting on Electroceramics (AMEC-9).

[34] Erturk A, Inman DJ, *Piezoelectric Energy Harvesting: Modelling and Application*. Sussex, UK: Wiley-Blackwell, 2011.
[35] Banks HT, Inman DJ, On damping mechanisms in beams. *Transactions of ASME, Journal of Applied Mechanics* 1991; **58**:716–723.
[36] Erturk A, Inman DJ, An experimentally validated bimorph cantilever model for piezoelectric energy harvesting from base excitations. *Smart Materials & Structures* 2009; **18**(2).
[37] Erturk A, Inman DJ, A distributed parameter electromechanical model for cantilevered piezoelectric energy harvesters. *Journal of Vibration and Acoustics-Transactions of the ASME* 2008; **130**(4).
[38] Erturk A, Inman DJ, On Mechanical Modeling of Cantilevered Piezoelectric Vibration Energy Harvesters. *Journal of Intelligent Material Systems and Structures* 2008; **19**(11):1311–1325.
[39] Erturk A, Inman DJ, Issues in mathematical modeling of piezoelectric energy harvesters. *Smart Materials & Structures* 2008; **17**(6).
[40] duToit NE, Wardle BL, Experimental verification of models for microfabricated piezoelectric vibration energy harvesters. *AIAA Journal* 2007; **45**(5):1126–1137.
[41] Adhikari S, Friswell MI, Inman DJ, Piezoelectric energy harvesting from broadband random vibrations. *Smart Materials & Structures* 2009; **18**(11):115005:1–7.
[42] Renno JM, Daqaq MF, Inman DJ, On the optimal energy harvesting from a vibration source. *Journal of Sound and Vibration* 2009; **320**(1-2):386–405.
[43] Vanmarcke EH, *Random fields*. Cambridge Mass.: MIT press, 1983.
[44] Papoulis A, Pillai SU, *Probability, Random Variables and Stochastic Processes*. 4th edition, Boston, USA: McGraw-Hill, 2002.
[45] Lin YK, *Probabilistic Theory of Structural Dynamics*. Ny, USA: McGraw-Hill Inc, 1967.
[46] Zhu J, *Stochastic Stability of Flow-Induced Vibration*. Ph.D. thesis, Ontario, Canada, 2008.
[47] Cai G, Wu C, Modeling of bounded stochastic processes. *Probabilistic Engineering Mechanics* 2004; **19**(3):197 – 203, fifth International Conference on Stochastic Structural Dynamics.
[48] Grigoriu M, *Applied Non-Gaussian Processes: Examples, Theory, Simulation, Linear Random Vibration, and Matlab Solutions*. New Jersey, USA: Prentice Hall, 1995.
[49] Ali SF, Adhikari S, Friswell MI, Narayanan S, The analysis of piezomagnetoelastic energy harvesters under broadband random excitations. *Journal of Applied Physics* 2011; **109**(7):074904:1–8.
[50] Adhikari S, Friswell MI, Litak G, Khodaparast HH, Design and analysis of vibration energy harvesters based on peak response statistics. *Smart Materials and Structures* 2016; **25**(6):065009:1–16.
[51] Nigam NC, *Introduction to Random Vibration*. Cambridge, Massachusetts: The MIT Press, 1983.
[52] Bolotin VV, *Random vibration of elastic systems*. The Hague: Martinus and Nijhoff Publishers, 1984.
[53] Roberts JB, Spanos PD, *Random Vibration and Statistical Linearization*. Chichester, England: John Wiley and Sons Ltd, 1990.
[54] Newland DE, *Mechanical Vibration Analysis and Computation*. New York: Longman, Harlow and John Wiley, 1989.
[55] Blevins RD, *Formulas for Natural Frequency and Mode Shape*. Malabar, FL, USA: Krieger Publishing Company, 1984.
[56] Adhikari S, Chowdhury R, The calibration of carbon nanotube based bio-nano sensors. *Journal of Applied Physics* 2010; **107**(12):124322:1–8.
[57] Meirovitch L, *Principles and Techniques of Vibrations*. New Jersey: Prentice-Hall International, Inc., 1997.

Appendix A. Reduced-order model for Euler-Bernoulli beams

Appendix A.1. Free vibration analysis

The undamped natural frequencies (Hz) of the cantilever beam in (1) can be expressed as

$$f_j = \frac{\lambda_j^2}{2\pi}\sqrt{\frac{EI}{\rho_h A L^4}}, \quad j = 1, 2, 3, \cdots \tag{A.1}$$

where λ_j needs to be obtained by [55] solving the following transcendental equation

$$\cos\lambda \cosh\lambda + 1 = 0 \tag{A.2}$$

Solving this equation, the values of λ_j can be obtained as 1.8751, 4.69409, 7.8539 and 10.99557. For larger values of j, in general we have $\lambda_j = (2j-1)\pi/2$. The vibration mode shape corresponding to the j-th natural frequency can be expressed as

$$\phi_j(\xi) = (\cosh\lambda_j\xi - \cos\lambda_j\xi) - \left(\frac{\sinh\lambda_j - \sin\lambda_j}{\cosh\lambda_j + \cos\lambda_j}\right)(\sinh\lambda_j\xi - \sin\lambda_j\xi) \tag{A.3}$$

where

$$\xi = \frac{x}{L} \tag{A.4}$$

is the normalised coordinate along the length of the cantilever. For sensing applications we are primarily interested in the first few modes of vibration only.

Consider the attached bluff body of mass M at the end of the cantilevered resonator in Fig. 1. The boundary conditions with an additional mass of M at $x = L$ can be expressed as

$$Z(0,t) = 0, \quad Z'(0,t) = 0, \quad Z''(L,t) = 0, \quad \text{and} \quad EIZ'''(L,t) - M\ddot{Z}(L,t) = 0 \tag{A.5}$$

Here $(\bullet)'$ denotes derivative with respective to x and $(\dot{\bullet})$ denotes derivative with respective to t. It can be shown that (see for example [56]) the resonant frequencies are still obtained from Eq. (A.1) but λ_j should be obtained by solving

$$(\cos\lambda \sinh\lambda - \sin\lambda \cosh\lambda)\,\Delta M\,\lambda + (\cos\lambda \cosh\lambda + 1) = 0 \tag{A.6}$$

Here

$$\Delta M = \frac{M}{\rho_h AL} \tag{A.7}$$

is the ratio of the tip mass and the mass of the cantilever. If the tip mass is zero, then one can see that Eq. (A.7) reduces to Eq. (A.2).

Appendix A.2. Equivalent single degree of freedom model

The equation of motion of the beam in (1) is a partial differential equation. This equation represents infinite number of degrees of freedom. The mathematical theory of linear partial differential equations is very well developed and the nature of solutions of the bending vibration is well understood. Considering a steady-state harmonic motion with frequency ω we have

$$Z(x,t) = z(x)\exp[\mathrm{i}\omega t] \tag{A.8}$$

where $\mathrm{i} = \sqrt{-1}$. Substituting this in the beam equation (1) we have

$$EI\frac{\mathrm{d}^4 z(x)}{\mathrm{d}x^4} + \mathrm{i}\omega\widehat{c}_1\frac{\mathrm{d}^4 z(x)}{\mathrm{d}x^4} - \rho_h A\omega^2 z(x) + \mathrm{i}\omega\widehat{c}_2 z(x) = 0 \tag{A.9}$$

Following the damping convention in dynamic analysis as in [57], we consider stiffness and mass proportional damping. Therefore, we express the damping constants as

$$\widehat{c}_1 = \alpha_c(EI) \quad \text{and} \quad \widehat{c}_2 = \beta_c(\rho A) \tag{A.10}$$

where α_c and β_c are stiffness and mass proportional damping factors. Substituting these, from Eq. (A.9) we have

$$EI\frac{\mathrm{d}^4 z(x)}{\mathrm{d}x^4} + \mathrm{i}\omega\left(\alpha_c EI\frac{\mathrm{d}^4 z(x)}{\mathrm{d}x^4} + \beta_c\rho_h A z(x)\right) - \rho_h A\omega^2 z(x) = 0 \tag{A.11}$$

The first part of the damping expression is proportional to the stiffness term while the second part of the damping expression is proportional to the mass term. The general solution of Eq. (A.11) can be expressed as a linear superposition of all the vibration mode shapes (see for example [57]). Vibration energy harvesters are often designed to operate within a frequency range which is close to first few natural frequencies only. Therefore, without any loss of accuracy, simplified lumped parameter models can be used to corresponding correct resonant behaviour. This can be achieved using energy methods or more generally using Galerkin approach.

Assuming a unimodal solution, the dynamic response of the beam can be expressed as

$$Z(x,t) = z_j(t)\phi_j(x), \quad j = 1,2,3,\cdots \tag{A.12}$$

Substituting this assumed motion into the equation of motion (1), multiplying by $\phi_j(x)$ and integrating by parts over the length one has

$$EIz_j(t)\int_0^L \phi_j^{''2}(x)\mathrm{d}x + \alpha_c EI\dot{z}_j(t)\int_0^L \phi_j^{''2}(x)\mathrm{d}x + \beta_c\rho_h A\dot{z}_j(t)\int_0^L \phi_j^2(x)\mathrm{d}x + \rho_h A\ddot{z}_j(t)\int_0^L \phi_j^2(x)\mathrm{d}x = 0 \tag{A.13}$$

Using the equivalent mass, damping and stiffness, this equation can be rewritten as

$$m_{eq_j}\ddot{z}_j(t) + c_{eq_j}\dot{z}_j(t) + k_{eq_j}z_j(t) = 0 \tag{A.14}$$

where the equivalent mass and stiffness terms are given by

$$m_{eq_j} = \rho_h A \int_0^L \phi_j^2(x)\mathrm{d}x = \rho_h AL \underbrace{\int_0^1 \phi_j^2(\xi)\mathrm{d}\xi}_{I_{1_j}} \tag{A.15}$$

$$k_{eq_j} = EI \int_0^L \phi_j^{''2}(x)\mathrm{d}x = \frac{EI}{L^3} \underbrace{\int_0^1 \phi_j^{''2}(\xi)\mathrm{d}\xi}_{I_{2_j}} \tag{A.16}$$

For the first mode of vibration ($j = 1$), substituting $\lambda_1 = 1.8751$, it can be shown that $I_{1_1} = 1$ and $I_{1_2} = 12.3624$. If there is a point mass of M at the tip of the cantilever, then the effective mass becomes

$$m_{eq_j} = \rho_h AL I_{1_j} + M \underbrace{\phi_j^2(1)}_{I_{3_j}} = \rho_h AL \left(I_{1_j} + \Delta M I_{3_j}\right) \tag{A.17}$$

For the first mode of vibration it can be shown that $I_{3_1} = 4$. The equivalent single degree of freedom model given by Eq. (A.14) is used in the rest of the paper. However, the expression derived here are general and can be used if higher modes of vibration were to be employed in energy harvesting.